

# Width dependent edge distribution of graphene nanoribbons unzipped from multiwall carbon nanotubes

Z. F. Zhong, H. L. Shen, R. X. Cao, L. Sun, K. P. Li, X. R. Wang, and H. F. Ding\*

Citation: *J. Appl. Phys.* **113**, 174307 (2013); doi: 10.1063/1.4803701

View online: <http://dx.doi.org/10.1063/1.4803701>

View Table of Contents: <http://aip.scitation.org/toc/jap/113/17>

Published by the [American Institute of Physics](#)

---

---

## Width dependent edge distribution of graphene nanoribbons unzipped from multiwall carbon nanotubes

Z. F. Zhong,<sup>1</sup> H. L. Shen,<sup>2</sup> R. X. Cao,<sup>1</sup> L. Sun,<sup>1</sup> K. P. Li,<sup>1</sup> X. R. Wang,<sup>2</sup> and H. F. Ding<sup>1,a)</sup>

<sup>1</sup>National Laboratory of Solid State Microstructures and Department of Physics, Nanjing University, 22 Hankou Road, Nanjing 210093, People's Republic of China

<sup>2</sup>National Laboratory of Solid State Microstructures and School of Electronic Science and Engineering, Nanjing University, 22 Hankou Road, Nanjing 210093, People's Republic of China

(Received 15 January 2013; accepted 16 April 2013; published online 6 May 2013)

We present the width dependent study of edge distribution of graphene nanoribbons unzipped from multi-wall nanotubes. The partial unzipping of the carbon nanotubes yields a mixture of carbon nanotubes and nanoribbons. Comparing atomic resolution images of scanning tunneling microscopy with the lattice of graphene, the edge structures of nanoribbons are identified. Below 10 nm, the edges are closer to armchair type. Above 20 nm, the ribbons prefer to have edges close to zigzag type. In between, a more random distribution of the edges is found. The findings are of potential usages for the edge control in graphene nanoribbon based applications. © 2013 AIP Publishing LLC. [<http://dx.doi.org/10.1063/1.4803701>]

### I. INTRODUCTION

Recently, a two-dimensional material with atomically thin carbon layer, graphene has attracted considerable attention due to its unique band structure and outstanding electrical properties.<sup>1–3</sup> Its electron transport can be described by the Dirac equation and its charge carriers are mimic massless Dirac fermions.<sup>4</sup> In addition, graphene has excellent chemical and mechanical stability and can present ballistic transport property at room temperature.<sup>5</sup> The above features make graphene a promising material for various applications. In real applications like electronic circuit, graphene often needs to be patterned into ribbons with nanometer in width, i.e., graphene nanoribbons (GNRs). GNRs are quasi-1D graphene nanostructures. Their properties strongly depend on both their width and edge structure.<sup>6–15</sup> For instance, localized states are found at the edges with energies close to the Fermi level in ribbons with zigzag edges.<sup>6,8</sup> A metallic edge state is known to prevent a band gap from opening.<sup>8</sup> Meanwhile, armchair nanoribbons, where edges orient 30° or 90° with respect to the zigzag direction, exhibit an oscillatory gap dependence on ribbon width.<sup>9–11</sup> The edge states are predicted to be absent for armchair nanoribbons.<sup>12</sup> Moreover, in zigzag nanoribbons, a magnetic ordering is predicted and allowed to split the edge states, resulting in an opposite magnetic coupling between two sides of the edges.<sup>13,14</sup> The armchair nanoribbons, however, are predicted to be nonmagnetic. The rich properties of GNRs make them a versatile material for new device design providing that their width and edge can be well controlled.

Several interesting methods, including the lithographic, chemical, and sonochemical methods, have been developed to fabricate GNRs.<sup>16–23</sup> Recently, a simple but highly efficient unzipping approach for the production of nanoribbons from pristine multiwall nanotubes (MWNTs) is reported.<sup>24</sup>

The unzipped narrow nanoribbons show nearly atomically smooth edges and a high conductance of up to  $5e^2/h$ . This simple and reliable approach makes nanoribbons easily accessible for exploring their potential applications. Since the property of GNR strongly depends on its width and edge structure, it would be highly desirable to explore the detailed edge information and its correlation with the ribbon width.

In this paper, we present the width dependent edge study of GNRs unzipped from MWNTs with scanning tunneling microscopy (STM). Owing to its atomic resolution, STM provides one of the best tools to explore the edge structures of GNRs.<sup>6</sup> By comparing the atomic resolution images of STM with the lattice structure of graphene, the edge structures of the nanoribbons are identified. The GNRs prefer to have edge structure close to the armchair type when their widths are below 10 nm. Above 20 nm, the opposite behavior is found, and the ribbons have edges close to the zigzag type. In between, a more random distribution of the edges is found. These findings could be useful for the edge control in GNR based applications.

### II. EXPERIMENTAL TECHNIQUES

In our study, the nanoribbons are fabricated by unzipping pristine MWNTs according to a method that has been reported. MWNTs were initially heated in air at 500 °C, which is a mild condition known to remove impurities and etch/oxidize MWNTs at defect sites and ends without oxidizing the pristine sidewall of the nanotubes. The nanotubes were then dispersed in a 1,2-dichloroethane (DCE) organic solution of poly(m-phenylenevinylene-co-2,5-dioctoxy-p-phenylenevinylene) (PmPV) by sonication, during which the nanotubes were found to be unzipped into nanoribbons. An Au(111) crystal was submerged into the freshly prepared solutions for ~2 h to obtain a certain amount of GNR deposition. After drying, the sample was transferred into an ultra-high vacuum (UHV) chamber which is equipped with a low temperature STM. The sample was initially outgassed in

<sup>a)</sup>Author to whom correspondence should be addressed. Electronic mail: hfding@nju.edu.cn

UHV condition at 200 °C for 30 min and further annealed at 500 °C for 60 min. After that it was transferred into the STM stage for imaging at 4.8 K.

### III. RESULTS AND DISCUSSION

Figure 1(a) presents a typical atomic force microscopy image of the unzipped GNRs after drying a prepared solution on a Si substrate which is covered by a thin silicon oxide layer. It shows 500 nm to a few  $\mu\text{m}$  long wires with different contrasts. The finding of wires with different contrasts shows that the nanoribbons are partially unzipped, similar as reported in Ref. 21. The wires with stronger contrast (thicker) are remaining nanotubes. And the wires with a dimmer contrast (thinner) are the unzipped nanoribbons. Interestingly, we find some of the nanoribbons are partially unzipped themselves (see the area marked by the white circle). The edge structures of the nanoribbons depend on both the types of the nanotubes and the directions that they are unzipped along. For instance, the unzipping of a zigzag/armchair nanotube along its tube axis [unzipping along the blue dash line shown in Figures 1(b) and 1(c)] will yield nanoribbons with armchair/zigzag edge, respectively. Originated from the same carbon nanotubes, if the unzipping directions are different [see the blue and red dashed lines in Figure 1(b)], the obtained GNRs will have different edges.

Figure 2(a) presents a typical image of a GNR. It shows two parallel and straight edges with the direction marked by the edge line. The scanning direction is from bottom to top. The gold surface is partially covered by small molecules remained from the chemical treatment. These molecules sometimes caused the tip instability and resulted artifacts such as jumping lines as shown in Figure 2(a) and its line profile in Figure 2(b). The line profile across the nanoribbon as marked by the blue line shows the GNR is about 0.4 nm above the Au(111) surface, evidence that the GNR is single

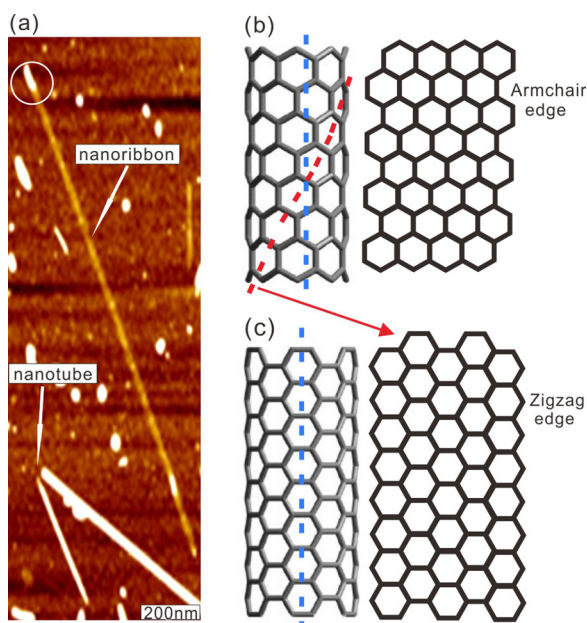


FIG. 1. (a) Atomic force microscopy image of GNR and carbon nanotube. (b) and (c) Models of the unzipping carbon nanotubes for armchair- and zigzag-GNRs, respectively.

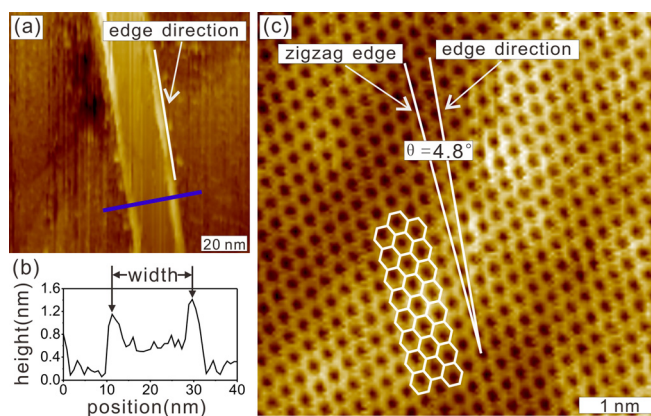


FIG. 2. Typical STM images of a single layer GNR. (a) Morphology of GNR. (b) Line profile across the GNR as marked by the blue line in (a). (c) Atomic resolved image of the same GNR in (a). The white honeycombs are lattice of GNR with zigzag edge. The comparison of the zigzag edge and the edge lines shown in (a) yields the edge direction of the GNR. The imaging conditions are 1 V, 1 nA.

layer (the height of a single step in graphite is 0.34 nm). The width of the GNR is about 20 nm. The stronger contrasts at GNR edges suggest the edges are bended, making it difficult to identify the edge structure directly. A zoomed (atomic resolution) image, Figure 2(c), shows an almost perfect honeycomb structure, a hole surrounded by 6 carbon atoms. The imaging conditions are 1 V, 1 nA. The holes form a hexagonal pattern. The almost clean and defect free surface suggests the GNRs may have the self-cleaning and self-reknitting capability similar as reported for graphene.<sup>25</sup> To identify the structures, we compare the STM image with the lattice of GNR with zigzag edge as marked by the white grids. Good agreements can be obtained. Some mismatches are also expected as the GNR surface is not perfectly flat due to the underlying small molecules. By comparing the atomic resolution image with the lattice model, we can find the edge of the GNR has an angle of  $\theta = 4.8^\circ$  with respect to the zigzag edge. As the holes are easier to be resolved in STM imaging and the zigzag edge is always parallel with the edge of hexagon formed by the holes, we also use the edge of the hexagon as the reference line as marked in Figure 2(c).

As the GNRs are unzipped from MWNTs, some of the GNRs are double or multi-layers.<sup>26</sup> Figure 3(a) shows a typical image of double layer GNR at the position near its edge. Its top layer is about 0.7 nm above the Au(111) surface.

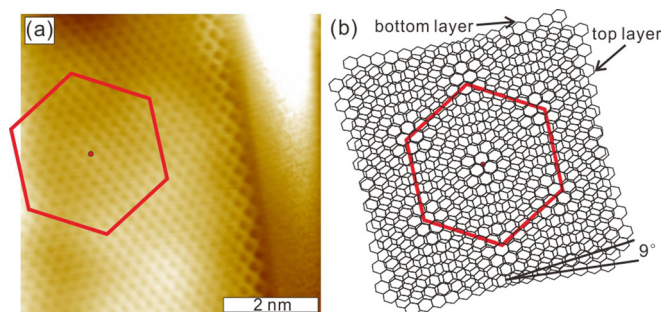


FIG. 3. (a) Typical STM image of a double layer GNR. The red hexagon marks the moiré pattern caused by the relative rotation of the bottom and top lattices. (b) Constructed model according to the moiré pattern shown in (a). The model shows that the rotation angle between two lattices is  $9^\circ$ .

Despite its double layer structure, the GNR shows only one pair of parallel edges, suggesting that the physical unzipping angles for the top and bottom layers are the same. Following the above procedure, we find that the edge of the top layer has an angle of  $\theta = 26.2^\circ$  with respect to the zigzag direction. Interestingly, we find there is a moiré pattern (marked by the red hexagon) besides the atomic structures. The existence of the moiré pattern suggests the lattices of the bottom and top layers orient differently. To obtain the edge structure of the bottom layer, we constructed a model based on the rotation of two graphene lattices, see Figure 3(b). The best fitting of the moiré pattern requires a rotation angle of  $9^\circ$  between these two lattices. As physically the edges of the top and bottom layers are parallel, we can derive that the edges of the bottom layer have an angle of  $\theta = 60^\circ - (26.2 + 9)^\circ = 24.8^\circ$  with respect to the zigzag direction. Thus, the edge structure of the bottom layer is also obtained. Interestingly, we find the top/bottom-layer have similar edge angles with respect to the zigzag direction for the double-layer GNR. The edges of the top/bottom layers have an angle of  $26.2^\circ/24.8^\circ$  with respect to the zigzag direction, respectively. Similar observations were also reported in Ref. 26, where the edges of the top/bottom layer have an angle of  $24^\circ/23^\circ$  ( $37^\circ$  in the original text) with respect to the zigzag direction in a double layer GNR and  $28^\circ/29^\circ$  ( $31^\circ$  in the original text) for the other one.

With the above discussed methods, we explored the width and the edge distribution of the GNRs unzipped from MWNTs. In the GNRs we studied, 4/6/9 out of 19 were single /double /multi-layer GNRs, respectively. The layer number of GNRs was estimated according to the height of the GNRs. We found that the width of the nanoribbons varied from 4 to 26 nm and the edges seemed to be randomly distributed varying from zigzag- to armchair-edge, in good agreement with previously reported results.<sup>26</sup> However, when we plotted the edge structure (only the edges of the top layers were included for the double layer and multilayer

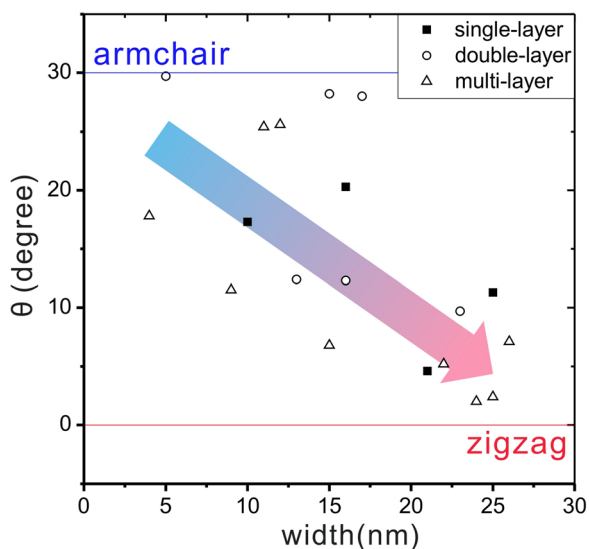


FIG. 4. Statistical distribution of the angle between edge direction and zigzag direction of the top layer in GNRs. The square/circle/triangle symbols represent single/double/multi-layer GNRs, respectively. The arrow is a guide for eyes.

GNRs) as a function of GNR width, Figure 4, an interesting tendency was found. Below 10 nm, the edges are found to be closer to armchair type. Above 20 nm, the ribbons prefer to have edges close to zigzag type. In between, a more random distribution of the edges is found. This may be related to the diameter dependent strain in NTs. The density functional theory (DFT) calculations show that the edge energy of armchair-GNR is lower than that of zigzag-GNR (about 20% lower) given the same ribbon width.<sup>27–29</sup> Thus, the total energy of the armchair-GNR is generally lower. However, the unzipping from the nanotube also involves the kinetics. From the unzipping model shown in Figure 1, we can find that the unzipping for GNRs with zigzag edge requires less bond-breaking in comparison with the unzipping for GNRs with armchair edge. Therefore, the energy barrier to form zigzag-GNR is expected to be lower without the influence of the strain. This may explain why wider GNRs prefer to have edges closer to zigzag type as the strain is negligible. The strain of NT with smaller diameter, however, is relatively large.<sup>22,30</sup> It may change the barrier shape or add extra energy to cross the higher barrier and bring the system to lower energy state, i.e., the armchair-GNR. The strain decreases with increasing diameter of the NT, leading to a transition from GNRs with armchair edges towards GNRs with zigzag edges as we observed experimentally. We note that the same trend is found when the bottom layer edges of the double-layer GNRs are included as we found the edges of the top and the bottom layer have similar orientations with respect to the zigzag direction.

#### IV. CONCLUSIONS

In summary, utilizing scanning tunneling microscopy, we investigated the width dependent edge distribution of GNRs unzipped from multi-wall nanotubes. By comparing the atomic resolution STM images with the graphene lattice, the edge structure of the single layer GNR is determined. With the observed moiré pattern, the rotation angle of the bottom and top lattices of the double layer GNR can also be resolved. Below 10 nm, the edges of the GNRs are found to be closer to armchair type. Above 20 nm, the ribbons prefer to have edges close to zigzag type. In between, a more random distribution of the edges is found. The interesting findings could be explained by the diameter dependent strain relief of carbon nanotubes. These findings are of usages for the edge control in graphene nanoribbon based applications.

#### ACKNOWLEDGMENTS

This work was supported by the State Key Programme for Basic Research of China (Grant No. 2010CB923401), NSFC (Grants Nos. 10834001, 10974087, and 11023002), Natural Science Foundation of Jiangsu (Grant No. BK2012300), and PAPD.

<sup>1</sup>K. S. Novoselov, A. K. Geim, S. V. Morozov, D. Jiang, M. I. Katsnelson, I. V. Grigorieva, S. V. Dubonos, and A. A. Firsov, *Nature* **438**, 197 (2005).

- <sup>2</sup>S. Stankovich, D. A. Dikin, G. H. B. Dommett, K. M. Kohlhaas, E. J. Zimmey, E. A. Stach, R. D. Piner, S. T. Nguyen, and R. S. Ruoff, *Nature* **442**, 282 (2006).
- <sup>3</sup>S. Ghosh, D. L. Nika, E. P. Pokatilov, and A. A. Balandin, *New J. Phys.* **11**, 095012 (2009).
- <sup>4</sup>A. H. Castro Neto, F. Guinea, N. M. R. Peres, K. S. Novoselov, and A. K. Geim, *Rev. Mod. Phys.* **81**, 109 (2009).
- <sup>5</sup>A. K. Geim and K. S. Novoselov, *Nature Mater.* **6**, 183 (2007).
- <sup>6</sup>C. Tao, L. Jiao, O. V. Yazyev, Y.-C. Chen, J. Feng, X. Zhang, R. B. Capaz, J. M. Tour, A. Zettl, S. G. Louie, H. Dai, and M. F. Crommie, *Nat. Phys.* **7**, 616 (2011).
- <sup>7</sup>Y. W. Son, M. L. Cohen, and S. G. Louie, *Nature* **444**, 347 (2006).
- <sup>8</sup>K. Nakada, M. Fujita, G. Dresselhaus, and M. S. Dresselhaus, *Phys. Rev. B* **54**, 17954 (1996).
- <sup>9</sup>M. Ezawa, *Phys. Rev. B* **73**, 045432 (2006).
- <sup>10</sup>L. Brey and H. A. Fertig, *Phys. Rev. B* **73**, 235411 (2006).
- <sup>11</sup>H. Zheng, Z. F. Wang, T. Luo, Q. W. Shi, and J. Chen, *Phys. Rev. B* **75**, 165414 (2007).
- <sup>12</sup>M. Fujita, K. Wakabayashi, K. Nakada, and K. Kusakabe, *J. Phys. Soc. Jpn.* **65**, 1920 (1996).
- <sup>13</sup>H. Lee, Y.-W. Son, N. Park, S. Han, and J. Yu, *Phys. Rev. B* **72**, 174431 (2005).
- <sup>14</sup>Y.-W. Son, M. L. Cohen, and S. G. Louie, *Phys. Rev. Lett.* **97**, 216803 (2006).
- <sup>15</sup>L. Zhu, J. Wang, T. Zhang, L. Ma, C. W. Lim, F. Ding, and X. C. Zeng, *Nano Lett.* **10**, 494 (2010).
- <sup>16</sup>L. Jiao, L. Zhang, X. Wang, G. Diankov, and H. Dai, *Nature* **458**, 877 (2009).
- <sup>17</sup>D. V. Kosynkin, A. L. Higginbotham, A. Sinitskii, J. R. Lomeda, A. Dimiev, B. K. Price, and J. M. Tour, *Nature* **458**, 872 (2009).
- <sup>18</sup>Z. Zhang, Z. Sun, J. Yao, D. V. Kosynkin, and J. M. Tour, *J. Am. Chem. Soc.* **131**, 13460 (2009).
- <sup>19</sup>A. G. Cano-Márquez, F. J. Rodríguez-Macías, J. Campos-Delgado, C. G. Espinosa-González, F. Tristán-López, D. Ramírez-González, D. A. Cullen, D. J. Smith, M. Terrones, and Y. I. Vega-Cantú, *Nano Lett.* **9**, 1527 (2009).
- <sup>20</sup>A. L. Elías, A. R. Botello-Méndez, D. Meneses-Rodríguez, V. Jehová González, D. Ramírez-González, L. Ci, E. Muñoz-Sandoval, P. M. Ajayan, H. Terrones, and M. Terrones, *Nano Lett.* **10**, 366 (2010).
- <sup>21</sup>W. S. Kim, S. Y. Moon, S. Y. Bang, B. G. Choi, H. Ham, T. Sekino, and K. B. Shim, *Appl. Phys. Lett.* **95**, 083103 (2009).
- <sup>22</sup>J. Wang, L. Ma, Q. Yuan, L. Zhu, and F. Ding, *Angew. Chem., Int. Ed.* **50**, 8041 (2011).
- <sup>23</sup>L. Ma, J. Wang, and F. Ding, *Angew. Chem., Int. Ed.* **51**, 1161 (2012).
- <sup>24</sup>L. Jiao, X. Wang, G. Diankov, H. Wang, and H. Dai, *Nat. Nanotechnol.* **5**, 321 (2010).
- <sup>25</sup>R. Zan, Q. M. Ramasse, U. Bangert, and K. S. Novoselov, *Nano Lett.* **12**, 3936 (2012).
- <sup>26</sup>L. Xie, H. Wang, C. Jin, X. Wang, L. Jiao, K. Suenaga, and H. Dai, *J. Am. Chem. Soc.* **133**, 10394 (2011).
- <sup>27</sup>S. Jun, *Phys. Rev. B* **78**, 073405 (2008).
- <sup>28</sup>P. Koskinen, S. Malola, and H. Häkkinen, *Phys. Rev. Lett.* **101**, 115502 (2008).
- <sup>29</sup>B. Huang, M. Liu, N. Su, J. Wu, W. Duan, B.-L. Gu, and F. Liu, *Phys. Rev. Lett.* **102**, 166404 (2009).
- <sup>30</sup>O. Gülseren, T. Yildirim, and S. Ciraci, *Phys. Rev. B* **65**, 153405 (2002).